Monosodium Urate Contributes to Retinal Inflammation and Progression of Diabetic Retinopathy

Menaka C. Thounaojam,[1] Annalisa Montemari,[2] Folami L. Powell,[3] Prerana Malla,[1] Diana R. Gutsaeva,[1] Alessandra Bachettoni,[4] Guido Ripandelli,[5] Andrea Repossi,[6] Amany Tawfik,[7] Pamela M. Martin,[3] Francesco Facchiano,[8] and Manuela Bartoli[1]

Diabetes 2019;68:1014–1025 | https://doi.org/10.2337/db18-0912

We have investigated the contributing role of monosodium urate (MSU) to the pathological processes associated with the induction of diabetic retinopathy (DR). In human postmortem retinas and vitreous from donors with DR, we have found a significant increase in MSU levels that correlated with the presence of inflammatory markers and enhanced expression of xanthine oxidase. The same elevation in MSU levels was also detected in serum and vitreous of streptozotocin-induced diabetic rats (STZ-rats) analyzed at 8 weeks of hyperglycemia. Furthermore, treatments of STZ-rats with the hypouricemic drugs allopurinol (50 mg/kg) and benzbromarone (10 mg/kg) given every other day resulted in a significant decrease of retinal and plasma levels of inflammatory cytokines and adhesion factors, a marked reduction of hyperglycemia-induced retinal leukostasis, and restoration of retinal blood-barrier function. These results were associated with effects of the hypouricemic drugs on downregulating diabetes-induced levels of oxidative stress markers as well as expression of components of the NOD-like receptor family pyrin domain-containing protein 3 (NLRP3) inflammasome such as NLRP3, Toll-like receptor 4, and interleukin-1β. The outcomes of these studies support a contributing role of MSU in diabetes-induced retinal inflammation and suggest that asymptomatic hyperuricemia should be considered as a risk factor for DR induction and progression.

Diabetic retinopathy (DR) is a progressive complication of type 1 and type 2 diabetes and the leading cause of legal blindness in adults (1). The identification of specific risk factors for DR is crucial to establish early therapeutic intervention and ultimately prevent vision loss. Poor glycemic control, hypertension, and hyperlipidemia are considered primary risk factors for the development and progression of DR (2). However, new evidence suggests that monitoring circulating levels of proinflammatory factors may hold better diagnostic value for the identification of patients at risk and/or for predicting disease progression (3,4).

Uric acid (UA) is a by-product of the purine metabolism (5), resulting from the oxidative catabolism of nucleic acids by xanthine oxidoreductase (XOD) (5). In normal physiological conditions, relatively high levels of UA are present in cells and in serum (6–11); however, when these levels reach and/or exceed 356 μmol/L (6 mg/dL) at physiological pH, UA undergoes nucleation in crystals of monosodium urate (MSU) (6,7,9). UA plasma levels >476 μmol/L (>8 mg/dL) cause gout, a human metabolic disorder and

[1]Department of Ophthalmology, Medical College of Georgia, Augusta University, Augusta, GA
[2]Istituto di Ricovero e Cura a Carattere Scientifico (IRCCS) Ospedale Pediatrico "Bambino Gesù," Rome, Italy
[3]Department of Biochemistry and Molecular Biology, Medical College of Georgia, Augusta University, Augusta, GA
[4]Department of Experimental Medicine and Pathology, University of Rome "LaSapienza," Rome, Italy
[5]Istituto di Ricovero e Cura a Carattere Scientifico (IRCCS) Fondazione G.B. Bietti, Rome, Italy
[6]Unità Operativa Complessa (UOC) Vitreoretina Ospedale San Carlo di Nancy, Rome, Italy
[7]Department of Oral Biology, Dental College of Georgia, Augusta University, Augusta, GA
[8]Department of Oncology and Molecular Medicine, Istituto Superiore di Sanità, Rome, Italy

Corresponding author: Manuela Bartoli, mbartoli@augusta.edu

Received 30 August 2018 and accepted 30 January 2019

This article contains Supplementary Data online at http://diabetes.diabetesjournals.org/lookup/suppl/doi:10.2337/db18-0912/-/DC1.

M.C.T. and A.M. equally contributed to the realization of these studies.

systemic inflammatory disease particularly affecting joints and kidneys (11,12).

Clinical studies have recently suggested that moderate "asymptomatic" hyperuricemia, defined as an elevation in serum UA levels ≥356 μmol/L, represents a risk factor for the development of cardiovascular disease, metabolic syndrome, and diabetic complications (8,13–15). The potential contributing role of UA in the induction and progression of these disease conditions has been linked to MSU function as an "alarmin" to activate the immune response and to promote auto (sterile) inflammation (16,17).

MSU has shown to be an activator of sterile inflammation through the induction of the NOD-like receptor family pyrin domain-containing protein 3 (NLRP3) inflammasome (17–20). Formation of this macromolecular complex in competent cells leads to cleavage/activation of interleukin-1β (IL-1β) and IL-18 (21). Toll-like receptor 4 (TLR4) and other TLRs functionally contribute to the inflammasome by promoting pro–IL-1β expression in a nuclear factor-κB–dependent manner (22,23).

In patients with diabetes, augmented UA serum levels have been correlated with the development of diabetic macroangiopathy (24), nephropathy (25–27), and neuropathy (28,29). To date, little is known on the specific contribution/correlation of UA to DR pathogenesis (30). However, evidence is provided that sterile inflammation is involved in DR pathogenesis and that this may implicate MSU activity (31).

In this study, we investigated the specific role of MSU in hyperglycemia-induced inflammatory processes in human and experimental DR by monitoring its levels in serum, vitreous, and retina of diabetic rodents and patients and by assessing the effects of UA-lowering drugs in preventing diabetes-induced retinal vessels inflammation and activation of the NLRP3 inflammasome.

RESEARCH DESIGN AND METHODS

Postmortem Human Samples

Deidentified postmortem human vitreous and retina samples were obtained from Georgia Eye Bank (Atlanta, GA) through its approved research program and by Augusta University Biosafety Committee. Supplementary Table 1 summarizes the demographics and clinical history available of the donors whose samples we used in our experiments.

Patients

The procedures in patients were conducted in compliance with the Declaration of Helsinki and according to protocols approved by the Ethical Committees of Clinica San Domenico, Ospedale San Giovanni dell' Addolorata (Rome, Italy) and Istituto Dermopatico dell'Immacolata, Istituto di Ricovero e Cura a Carattere Scientifico San Carlo, Rome Italy. Patients provided preoperative informed written consent and approved the use of the excised vitreous fluids for the presented studies. Diagnosis and staging of DR were made after complete ophthalmologic examination that included measurements of visual acuity (Early Treatment of Diabetic Retinopathy Study [ETDRS]), fluorescein angiography (FA), and optical coherence tomography.

In addition to the ophthalmological examination, the patients were asked to complete a questionnaire comprehensive of present and past comorbidities and treatments as well as questions pertaining to lifestyles, as summarized in Supplementary Table 2.

All patients were candidates for vitrectomy as a consequence of tractional retinal detachment or a nonclearing vitreous hemorrhage. Importantly, no technical changes to the surgical procedures were made to accommodate in any way the research protocol.

Human Vitreous Processing

Postmortem human vitreous samples were diluted (1:3) with PBS without calcium and magnesium and resuspended using a 26-gauge needle. Vitreous samples were briefly centrifuged at 2,000 rpm at 4°C, and supernatants were assessed for UA concentration as described below.

Undiluted vitreous samples (0.3–0.6 μL) were obtained from 18 patients undergoing pars plana vitrectomy. The control group consisted of nine patients who had undergone vitrectomy for the treatment of pucker or retinal detachment consequent to trauma. Vitreouses were collected undiluted by manual suction into a syringe through the aspiration line of the vitrectomy unit before the infusion line was opened. The samples were frozen at −80°C until processed for the different analyses.

Animals

All animal procedures were performed in agreement with the statement of the Association for Research in Vision and Ophthalmology for the humane use of animals in vision science and in compliance with approved institutional protocols. Animals were kept with a 12-h day/night light cycle and fed ad libitum. Adult male Sprague-Dawley rats (250–300 g), obtained from Envigo (Dublin, VA), were made diabetic by one intraperitoneal injection of streptozotocin (STZ) (65 mg/kg dissolved in 0.1 mol/L sodium citrate, pH 4.5) (Sigma-Aldrich, St. Louis, MO). Age-matched control rats received vehicle alone. Rats were considered to be diabetic (STZ-rats) when fasting blood glucose levels were ≥300 mg/dL. All animals were sacrificed after 8 weeks of hyperglycemia with an overdose of anesthesia, followed by thoracotomy.

Some STZ-rats received the hypouricemic drugs, allopurinol (50 mg/kg) or benzbromarone (10 mg/kg), which were administered every other day orally with sugar-/fat-free Jell-O mix for the 8-week duration of diabetes. The drugs' effective doses were established based on previously published protocols (32,33). Untreated STZ-rats received Jell-O mix alone. Blood glucose levels, body weights, and

several metabolic parameters for each experimental group are summarized in Supplementary Table 3.

UA and Uricase Activity Measurements

UA levels in vitreous of postmortem donors were assessed using a commercially available assay kit (BioAssay Systems, Hayward, CA) following the manufacturer's instructions. UA levels in vitreous from patients undergoing vitrectomy were measured using a kit (donated by Roche Diagnostic S.p.a., Milano, Italy) for the cobas 6000 analyzer (Roche Diagnostics). UA and uricase activity in rat vitreous and serum was measured using the Amplex Red Uric Acid/Uricase Assay Kit (Life Technologies, Carlsbad, CA).

Leukostasis

Leukocyte adhesion was determined as previously described (3). Rats were perfused with 10 mL PBS, followed by 10 mL FITC-labeled concanavalin A (ConA) lectin (40 μg/mL in PBS, pH 7.4) (Vector Laboratories, Burlingame, CA). Residual unbound ConA was removed by perfusion with PBS only. Eye globes were fixed with 4% paraformaldehyde. Flat-mounted retinas were observed by fluorescence microscopy, using a Zeiss Axioplan-2 microscope (Carl Zeiss, Göttingen, Germany) equipped with the Axiovision 4.7 software. The total number of adherent leukocytes per retina was counted in blind fashion.

Assessment of Blood-Retinal Barrier Integrity

Retinal vascular permeability in living animals was assessed as described before (34). Briefly, rats were anesthetized (ketamine, 100 mg/kg; xylazine, 30 mg/kg; and acepromazine, 10 mg/kg). Pupils were dilated using 1% tropicamide (Bausch & Lomb, Rochester, NY), and Goniovisc 2.5% (hypromellose; Sigma Pharmaceuticals, LLC, Monticello, IA) was applied liberally to retain surface moisture during imaging. Each animal was placed on the imaging platform of the Phoenix Micron III retinal imaging microscope (Phoenix Research Laboratories, Pleasanton, CA), and an intraperitoneal injection (80–100 μL) of fluorescein sodium (10% Lite) (Apollo Ophthalmics, Newport Beach, CA) was administered. Rapid acquisition of fluorescent images ensued for ~5 min. For a quantitative evaluation of blood-retinal barrier (BRB) integrity, we assessed albumin extravasation in rats after perfusion (34,35). Serum albumin levels were measured in the perfused retinal tissue by Western blot using anti-rat albumin antibody (Cell Signaling Technology, Danvers, MA).

Immunohistochemistry

Frozen retinal sections were fixed in 4% paraformaldehyde, followed by incubation at 4°C overnight with the following primary antibodies: anti-UA (Abcam, Cambridge, MA), anti-XOD (Novus Biologicals, Littleton, CO), anti-glial fibrillary acidic protein (GFAP) (Cayman Chemical, Ann Arbor, MI), and anti–4-hydroxynonenal (4-HNE) (Abcam). After washing, the slides were incubated for 1 h with IgG-conjugated Alexa Fluor-488 secondary antibodies (Molecular Probes-Life Technologies, Grand Island, NY). Some sections were colabeled with isolectin B4 to identify the retinal vasculature. Mounted sections were examined by epifluorescence using a Zeiss Axioplan-2 microscope.

Protein Analysis

Immunoblotting was performed using the following antibodies: anti-NLRP3 (LifeSpan BioSciences, Seattle, WA), anti-TLR4 (Santa Cruz Biotechnology), anti-XOD (Novus Biologicals), and anti-intercellular adhesion molecule-1 (ICAM-1) (Abcam). Dot blot analysis was conducted to analyze immunoreactivity to 4-HNE (Abcam). After incubation with horseradish peroxidase–conjugated secondary antibody (GE Healthcare, Pittsburgh, PA), bands were detected using the enzymatic chemiluminescence reagent (ECL; GE Healthcare) or clarity ECL-Blotting substrate (Bio-Rad). Assessment of vascular endothelial growth factor (VEGF) protein levels was done using heparin affinity columns (Sigma-Aldrich) and Western blot analysis, as previously described (34).

Cytokines Assay

Tissue and plasma cytokine levels were determined using a customized Rat Mix and Match Cytokine ELISA strip assay (Signosis, Santa Clara, CA). Retinal tissue samples from different experimental groups were homogenized using 1× cell lysis buffer (Signosis), and total protein concentration was quantified using the Coomassie Plus (Bradford) Assay Kit. Samples containing equivalent amount of proteins were added to different wells individually coated with primary antibodies (tumor necrosis factor-α [TNF-α], transforming growth factor-β [TGF-β], IL-1β, IL-10, IL-17, and IL-6). Plates were processed according to the manufacturer's instructions and were read at 450 nm. Protein standards provided by the manufacturer were used to calculate each cytokine concentration and expressed as ng/mg of protein. Quantitative determination of IL-1β in human retinal extracts was performed using Human IL-1β Quantikine ELISA kit (R&D Systems, Minneapolis, MN).

Statistical Analysis

Graphs were prepared using Graph Pad Prism 3.0 software for Windows (Graph Pad Software, San Diego, CA). Data are shown as means ± SD. Statistical significance among experimental groups was established using one-way ANOVA, followed by the Bonferroni multiple-comparison test. Differences were considered significant when P was <0.05.

RESULTS

Increased Levels of UA in Retinal Extracts and Vitreous of Human DR Donors and Patients

We first analyzed UA levels in vitreous of human postmortem donors (Fig. 1*A*) and in patients undergoing pars

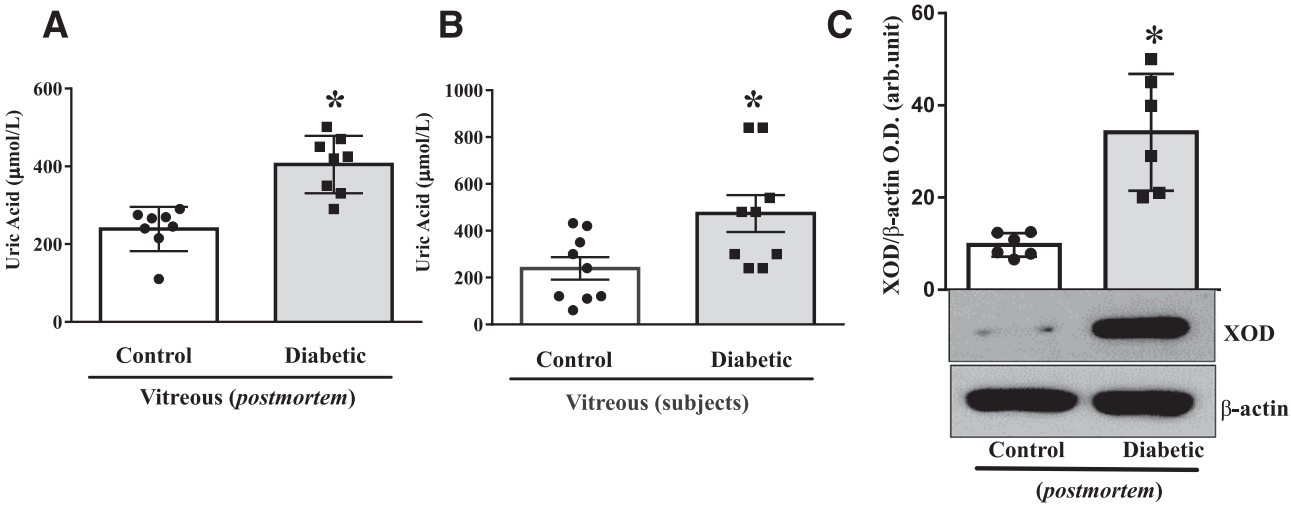

Figure 1—Assessment of UA and XOD levels in human retinas. *A*: UA levels in the vitreous of postmortem normoglycemic donors (Control) and donors with DR (Diabetic) are represented as a bar histogram. Data are means ± SD; $n = 8$. *$P < 0.001$ vs. control. *B*: UA levels in the vitreous of patients with DR (Diabetic) or control subjects without diabetes (Control) who underwent pars plana vitrectomy for retinal detachment or nonclearing vitreous hemorrhage. Data are means ± SD; $n = 9$. *$P < 0.01$ vs. Control. *C*: Western blot analysis of XOD-specific immunoreactivity in retinas of postmortem donors. Bar histograms represent measures of optical density (O.D.) of normalized vs. β-actin. Data are means ± SD; $n = 6$. *$P < 0.01$ vs. Control.

plana vitrectomy (Fig. 1*B*). In vitreous of human postmortem control donors without diabetes, UA was found at nonpathological concentration (237.5 ± 63.52 μmol/L), whereas in donors with DR, UA vitreous levels were significantly higher than the control donors ($P < 0.001$; $n = 8$) and at nucleation threshold levels (404.5 ± 73.64 μmol/L).

In vitreous of patients undergoing pars plana vitrectomy, UA levels were found at nonpathological concentration in control patients without diabetes (239.1 ± 142.80 μmol/L), whereas in vitreous of patients with DR, UA levels exceeded the nucleation threshold (473.3 ± 235.2 μmol/L) and were significantly higher than in control donors ($P < 0.01$; $n = 9$) (Fig. 1*B*).

Furthermore, we assessed the expression pattern of XOD, the rate-limiting enzyme leading to UA production. As shown in Fig. 1*C*, XOD protein levels, measured by immunoblotting, were significantly upregulated in retinal lysates of human postmortem donors with diabetes compared with control donors without diabetes ($P < 0.01$; $n = 6$).

Increased UA Levels in Serum, Vitreous, and Retina of STZ-Rats

In nonprimate mammals, UA undergoes the conversion to allantoin by uricase (urate oxidase). Because this enzyme can prevent the accumulation of UA in diabetic rats (36), we first assessed serum uricase activity in control and STZ-rats at 8 weeks of diabetes. We found that hyperglycemia increased uricase activity in STZ-rats compared with control normoglycemic rats ($P < 0.05$; $n = 6$) (Fig. 2*A*). However, despite this increase, UA serum levels were significantly augmented in STZ-rats compared with normoglycemic rats (412.4 ± 67.55 μmol/L vs. 75.5 ± 11.84 μmol/L; $P < 0.01$; $n = 6$) (Fig. 2*B*). Moreover, UA concentration measured in vitreous was also significantly upregulated in STZ-rats compared with control (370.6 ± 5 μmol/L vs. 42.3 ± 9.57 μmol/L; $P < 0.01$; $n = 6$) (Fig. 2*C*). Increased MSU deposition in diabetic retinas was also confirmed by immunohistochemical analysis using antibodies specifically recognizing MSU, which is the crystal form of UA. As shown in Fig. 2*D*, immunoreactivity to MSU was higher in retinas of STZ-rats compared with control rats. MSU accumulation was evident throughout all retinal layers and was also found around the retinal blood vessels and retinal pigmented epithelium (RPE) (Fig. 2*D*). Retinal UA was also determined in 6-week-old Akita mice, a genetic model of type 1 diabetes, in cryoslides, offered by A.T. (Supplementary Fig. 1).

Western blot and immunohistochemical analyses were conducted to assess the expression and immunolocalization of XOD in the different treatment groups. XOD-specific immunoreactivity was increased throughout the STZ-rat retinas and also localized in the retinal vasculature and the RPE (Fig. 2*E*). Immunoblotting analysis confirmed increased XOD protein levels in the diabetic compared with control retinas ($P < 0.05$; $n = 6$) (Fig. 2*F*).

Hypouricemic Drugs Diminish Hyperglycemia-Induced Retinal and Systemic Inflammation

To further establish a direct influence of UA on DR induction and progression, we determined the effects of hypouricemic drugs in preventing hyperglycemia-induced retinal inflammation and tissue damage during the early stages of DR. STZ-rats were treated with allopurinol,

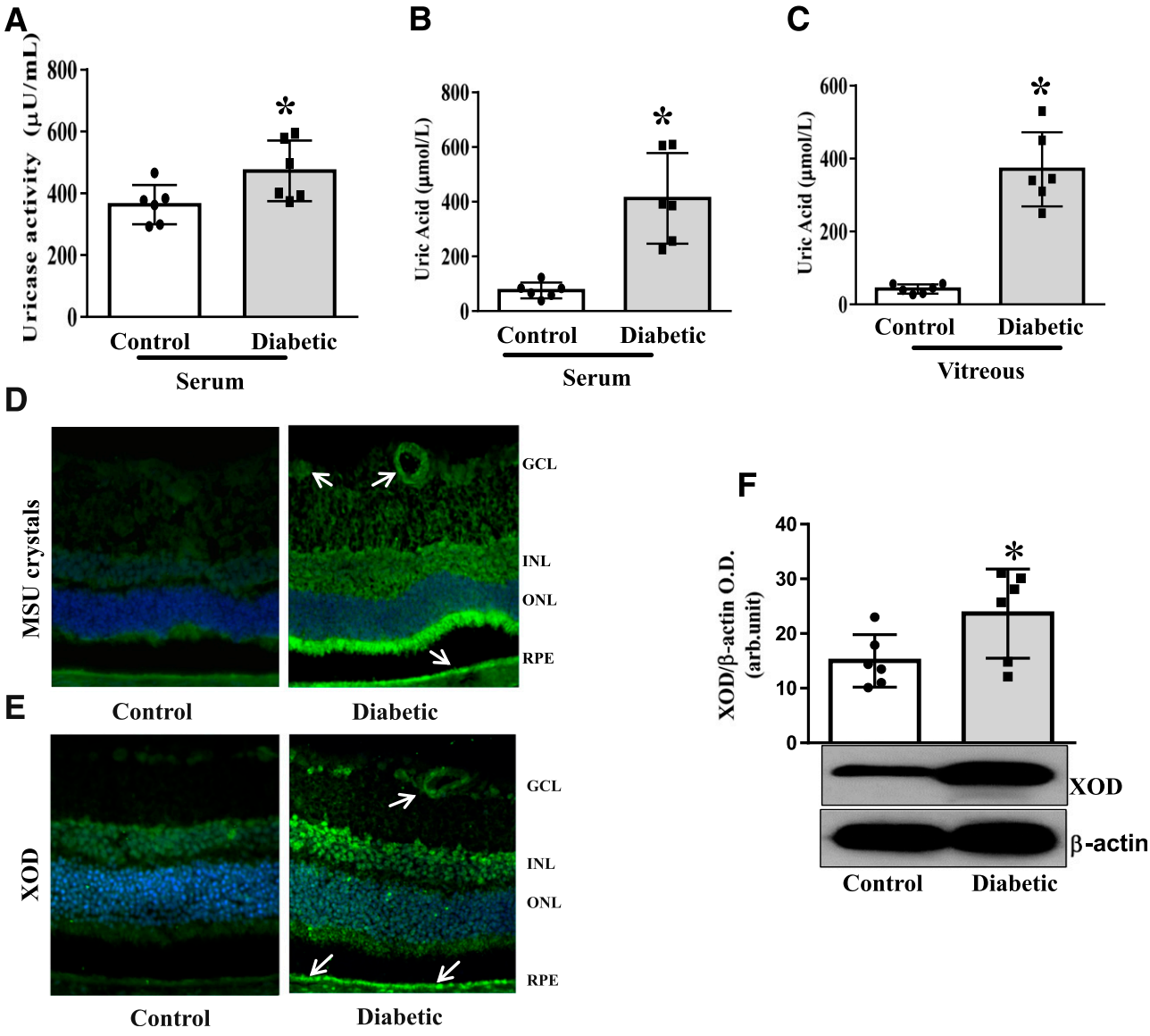

Figure 2— Assessment of UA and XOD levels in STZ-rats (Diabetic). *A*: Uricase activity in serum in control and STZ-rats. *$P < 0.05$ vs. Control. UA levels in serum (*B*) and vitreous (*C*) in control and STZ-rats. *$P < 0.01$ vs. Control. *D*: Representative images of immunohistochemical analysis of UA (green) in retinas from control and STZ-rats. *E*: Representative images of immunohistochemical analysis of XOD-specific immunoreactivity (green) in retinal vascular and RPE (white arrows) sections from control and STZ-rats. Nuclei were labeled with Hoechst 33342 (blue). GCL, ganglion cell layer; INL, inner nuclear layer; ONL, outer nuclear layer. *F*: XOD protein levels determined by Western blot analysis. Bar histograms are representative of measurements of the optical density (O.D.) of XOD-specific immunoreactivity of normalized vs. β-actin. Data are mean ± SD; $n = 6$. *$P < 0.05$ vs. Control.

a specific inhibitor of XOD (32), and benzbromarone, which enhances UA urinary excretion (33). As shown in Fig. 3*A*, both drugs significantly reduced serum levels of UA in STZ-rats ($P < 0.001$ for allopurinol and $P < 0.05$ benzbromarone; $n = 6$). Allopurinol had a more pronounced effect by decreasing serum UA as low as control rats (Fig. 3*A*), and differences between the two drugs were statistically significant ($P < 0.001$; $n = 6$). The reduction in UA levels in STZ-rats treated with these hypouricemic drugs also normalized uricase activity ($P < 0.01$; $n = 6$) (Fig. 3*B*). Treatments with allopurinol and benzbromarone, however, did not modify blood glucose and glycated hemoglobin (HbA_{1c}) levels in STZ-rats (Supplementary Table 3) but did normalize the levels of several metabolic parameters in STZ-rats, including alanine aminotransferase, aspartate transaminase, and cholesterol. Furthermore, treatment with allopurinol but not benzbromarone significantly reduced body weight loss in STZ-rats ($P < 0.05$) (Supplementary Table 3).

Using custom cytokine ELISA plate arrays, we further assessed the levels of several inflammatory cytokines in retinal extracts and plasma in response to the different treatments. Levels of IL-1β, IL-6, IL-17, TNF-α, and TGF-β were significantly elevated in retinal extracts ($P < 0.05$;

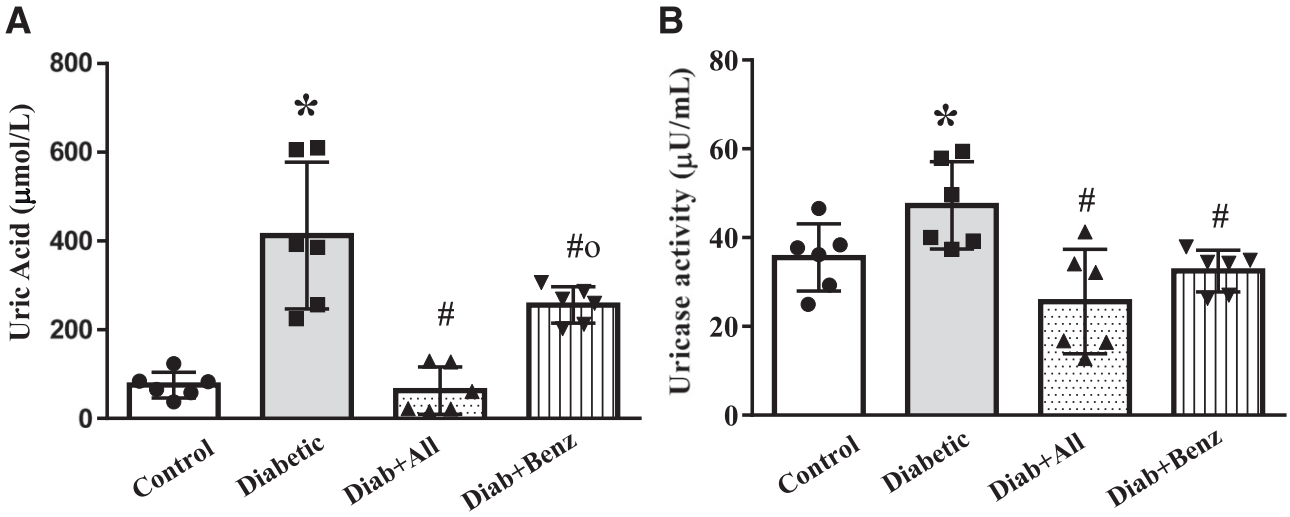

Figure 3—Effects of UA-lowering drugs on levels of UA and uricase activity. *A*: Levels of UA in serum of control rats (Control), STZ-rats (Diabetic), and STZ-rats receiving allopurinol (Diab+All) (#$P < 0.001$ vs. Diabetic) or benzbromarone (Diab+Benz) (#$P < 0.05$ vs. Diabetic). *$P < 0.001$ vs. Control; o$P < 0.001$ Diab+Benz vs. Diab+All. *B*: Uricase activity measured in serum of STZ-rats treated with allopurinol or benzbromarone (#$P < 0.01$ vs. Diabetic). Data are mean ± SD; $n = 6$.

$n = 6$) (Fig. 4) and plasma ($P < 0.05$; $n = 6$) (Supplementary Fig. 2) of STZ-rats compared with controls. This effect was blocked by treatment of STZ-rats with allopurinol or benzbromarone ($P < 0.05$; $n = 6$) (Fig. 4 and Supplementary Fig. 2). However, IL-10 protein levels were significantly downregulated in retina and plasma of STZ-rats compared with controls ($P < 0.05$; $n = 6$), and treatments with allopurinol or benzbromarone significantly increased IL-10 levels to control values (Fig. 4 and Supplementary Fig. 2).

Next, we determined the effect of UA-lowering drugs on hyperglycemia-induced retinal expression of VEGF and ICAM-1. VEGF expression was significantly increased in diabetic retinas compared with controls ($P < 0.001$; $n = 6$)

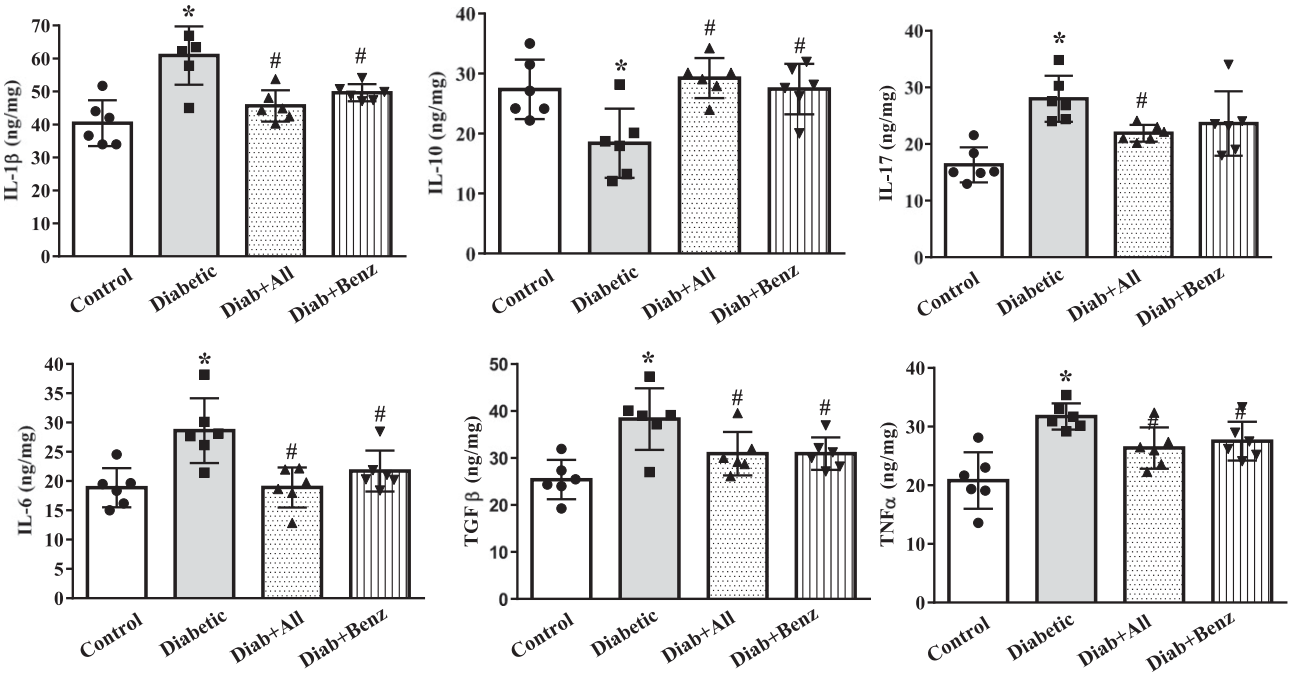

Figure 4—Effects of UA inhibition on cytokine profile in rat retinas and serum. Expression of IL-1β, IL-6, IL-17, IL-10, TNF-α, and TGF-β were evaluated in retinal tissue in control rats (Control), STZ-rats (Diabetic), and STZ-rats receiving allopurinol (Diab+All) or benzbromarone (Diab+Benz) using a customized ELISA kit. Data are mean ± SD; $n = 6$. *$P < 0.05$ vs. Control; #$P < 0.05$ vs. Diabetic.

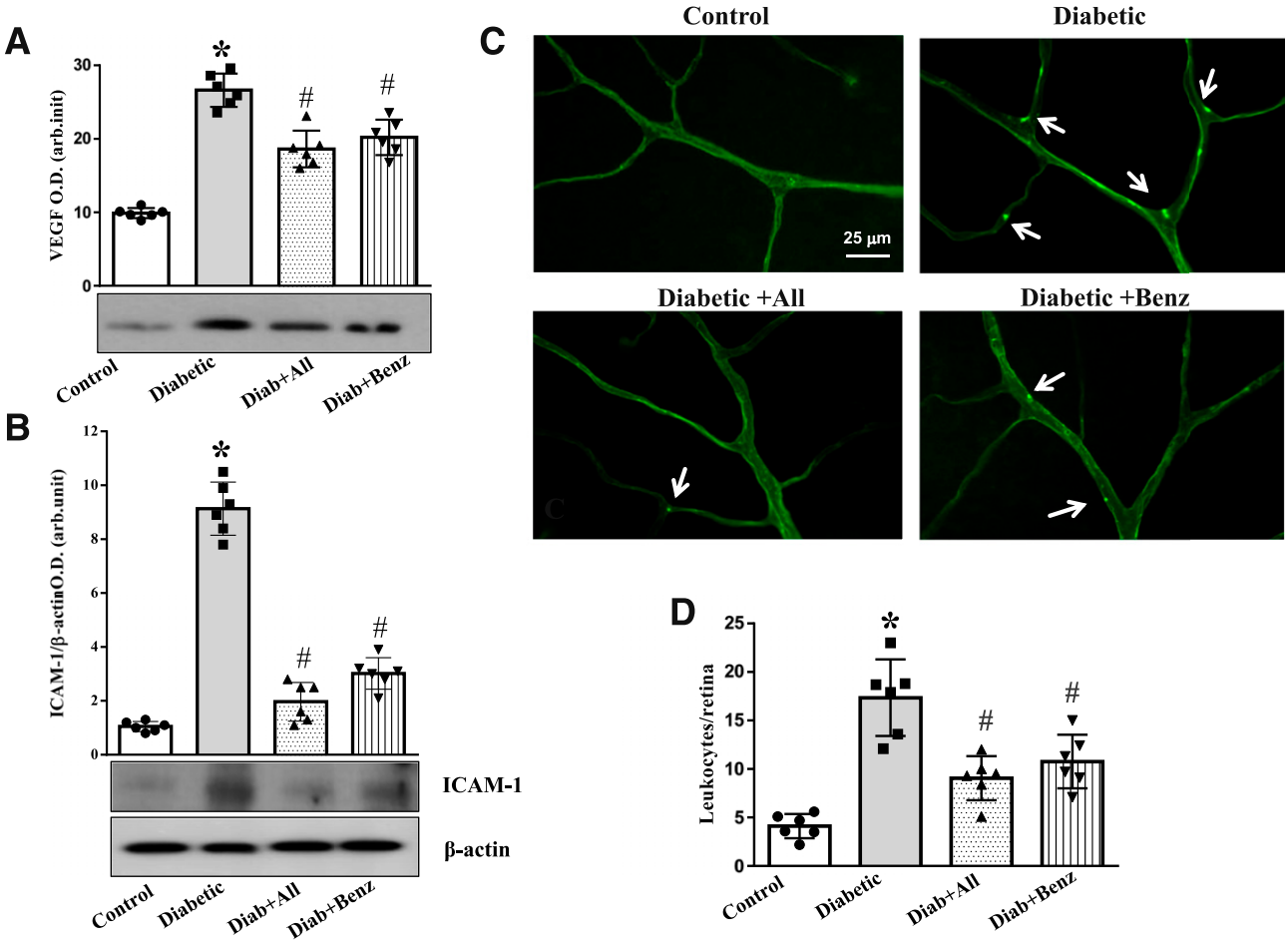

Figure 5—Effects of hypouricemic drugs on diabetes-induced VEGF and ICAM-1 expression and retinal leukostasis. *A*: VEGF protein levels determined by Western blot analysis in retinal tissue in control rats (Control), STZ-rats (Diabetic), and STZ-rats receiving allopurinol or benzbromarone (Diab+All and Diab+Benz, respectively). Bar histograms are representative of measurements of the optical density (O.D.) of VEGF-specific immunoreactivity. *$P < 0.001$ vs. Control; #$P < 0.001$ vs. Diabetic. *B*: ICAM-1 protein levels determined by Western blot analysis in retinal tissue in control rats (Control), STZ-rats (Diabetic), and STZ-rats receiving allopurinol (Diab+All) or benzbromarone (Diab+Benz). Bar histograms are representative of measurements of the optical density of ICAM-1–specific immunoreactivity normalized vs. β-actin. *$P < 0.001$ vs. Control; #$P < 0.001$ vs. Diabetic. *C*: Representative images of flat-mounted retinas stained with ConA to identify leukocytes adherent to retinal microvessels (white arrows). Scale bar = 25 μm. *D*: Quantification of number of adherent leukocytes per retina quantified in the different experimental groups. Data are mean ± SD; $n = 6$. *$P < 0.01$ vs. Control; #$P < 0.01$ vs. Diabetic.

(Fig. 5*A*). However, expression of VEGF in STZ-rats was significantly suppressed by treatments with allopurinol or benzbromarone ($P < 0.001$; $n = 6$) (Fig. 5*A*). ICAM-1 is one of key mediators of diabetes-induced retinal inflammation (37), and ICAM-1 upregulation leads to leukocyte adhesion (leukostasis) in the diabetic retina, an inflammatory event involved in progression of DR (38). In STZ-rat retinas, ICAM-1 expression was significantly upregulated compared with normoglycemic rats ($P < 0.001$; $n = 6$) (Fig. 5*B*); however, treatments with allopurinol or benzbromarone significantly reduced ICAM-1 expression in diabetic retinas ($P < 0.001$; $n = 6$) (Fig. 5*A*). In agreement with these data, the number of adherent leukocytes in the STZ-rat microvasculature was 4.8-fold higher than in normoglycemic rats ($P < 0.001$; $n = 6$) (Fig. 5*C* and *D*). Treatments of STZ-rats with allopurinol or benzbromarone significantly reduced the number of adherent leukocytes by 44.24% and 34.5%, respectively ($P < 0.01$; $n = 6$) (Fig. 5*D*), thus suggesting that UA contributes to leukostasis in the diabetic retina.

UA-Lowering Drugs Diminish Hyperglycemia-Induced BRB Breakdown in STZ-Rats

Breakdown of the BRB is an important pathological feature of DR (39,40). To assess the effects of UA-lowering drugs on the BRB, we performed FA in all the treatment groups. The obtained results show that allopurinol or benzbromarone significantly reduced fluorescein extravasation induced by hyperglycemia (Fig. 6*A*). This effect was also confirmed by measurements of albumin protein levels by immunoblotting in retinal extracts obtained from rats after perfusion. As shown in Fig. 6*B*, albumin levels were significantly elevated in retinas of STZ-rats compared with control rats ($P < 0.001$; $n = 6$). Allopurinol and

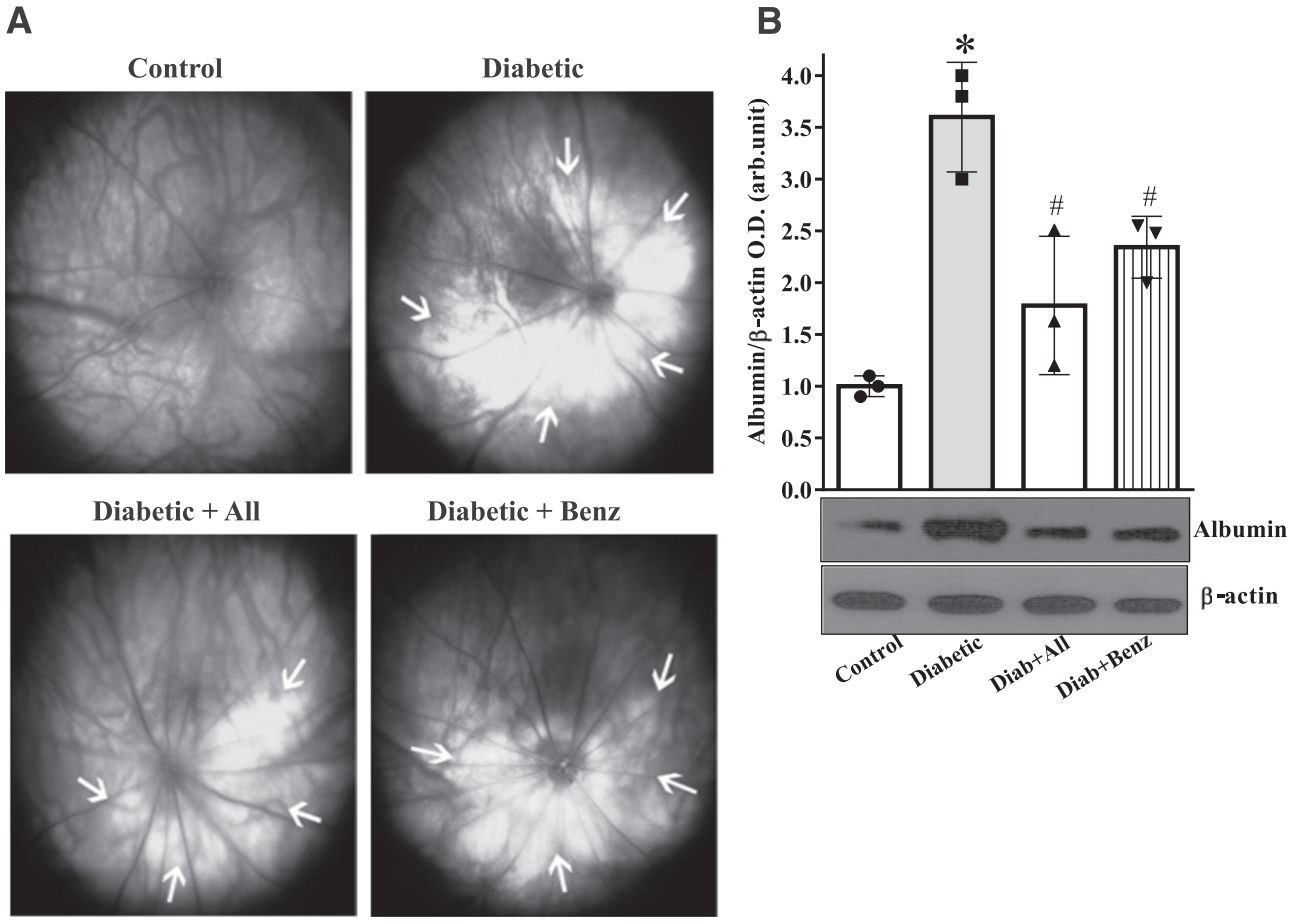

Figure 6—Effects of hypouricemic drugs on diabetes-induced BRB breakdown. *A*: Representative images of FA of control normoglycemic age-matched rats (Control), STZ-rats (Diabetic), and STZ-rats treated with allopurinol (Diab+All) or benzbromarone (Diab+Benz). Photographs were taken at constant intervals for every rat studied in each experimental group ($n = 6$). White arrows indicate the areas of vascular leakage. *B*: Western blot analysis assessing albumin protein levels in retinal extracts of perfused rats from the different experimental groups. The data are expressed as arbitrary units of optical density (O.D.) and normalized for the loading control β-actin. Data are mean ± SD; $n = 6$. *$P < 0.001$ vs. Control; #$P < 0.05$ vs. Diabetic.

benzbromarone both significantly decreased albumin levels in retinal extracts of STZ-rats ($P < 0.05$; $n = 6$), thus suggesting that limitation of UA production and accumulation in the diabetic retina, while halting retinal inflammation, also prevents hyperglycemia-induced breakdown of the BRB.

Hypouricemic Drugs Diminish Hyperglycemia-Induced Retinal Stress Markers

We further sought to determine the potential mechanism of action of UA in the diabetic retina by examining the effects of hypouricemic drugs on hyperglycemia-induced retinal oxidative stress, a major contributing factor for diabetes-induced retinal inflammation and progression to DR (3,41).

Detection of the lipid peroxidation by-product 4-HNE is used as an indicator of dysregulated lipid metabolism due to aberrant reactions between lipids and free radicals (42,43). Immunohistochemical analysis revealed that 4-HNE–specific immunoreactivity was significantly enhanced in the diabetic rat retina (Fig. 7*A*). Treatments with allopurinol or benzbromarone lowered 4-HNE–specific immunoreactivity (Fig. 7*A*). Dot blot analysis measuring 4-HNE levels confirmed the immunohistochemical data (Fig. 7*B*).

Finally, UA-lowering drugs decreased hyperglycemia-induced reactive gliosis as assessed by measures of GFAP immunoreactivity in STZ-rat retina compared with age-matched normoglycemic rat retina (Fig. 7*C*). Western blot analysis further confirmed these findings and showed that treatments of STZ-rats with allopurinol and benzbromarone significantly lowered GFAP expression in comparison with untreated STZ-rats ($P < 0.001$; $n = 6$) (Fig. 7*D*).

UA-Lowering Drugs Diminish Hyperglycemia-Induced NLRP3 Inflammasome Activation

Previous studies suggest that MSU-induced proinflammatory responses involve the activation of the sterile inflammation via NLRP3 inflammasome (17–20). To further investigate the specific contribution of UA to hyperglycemia-induced metabolic (sterile) inflammation, we

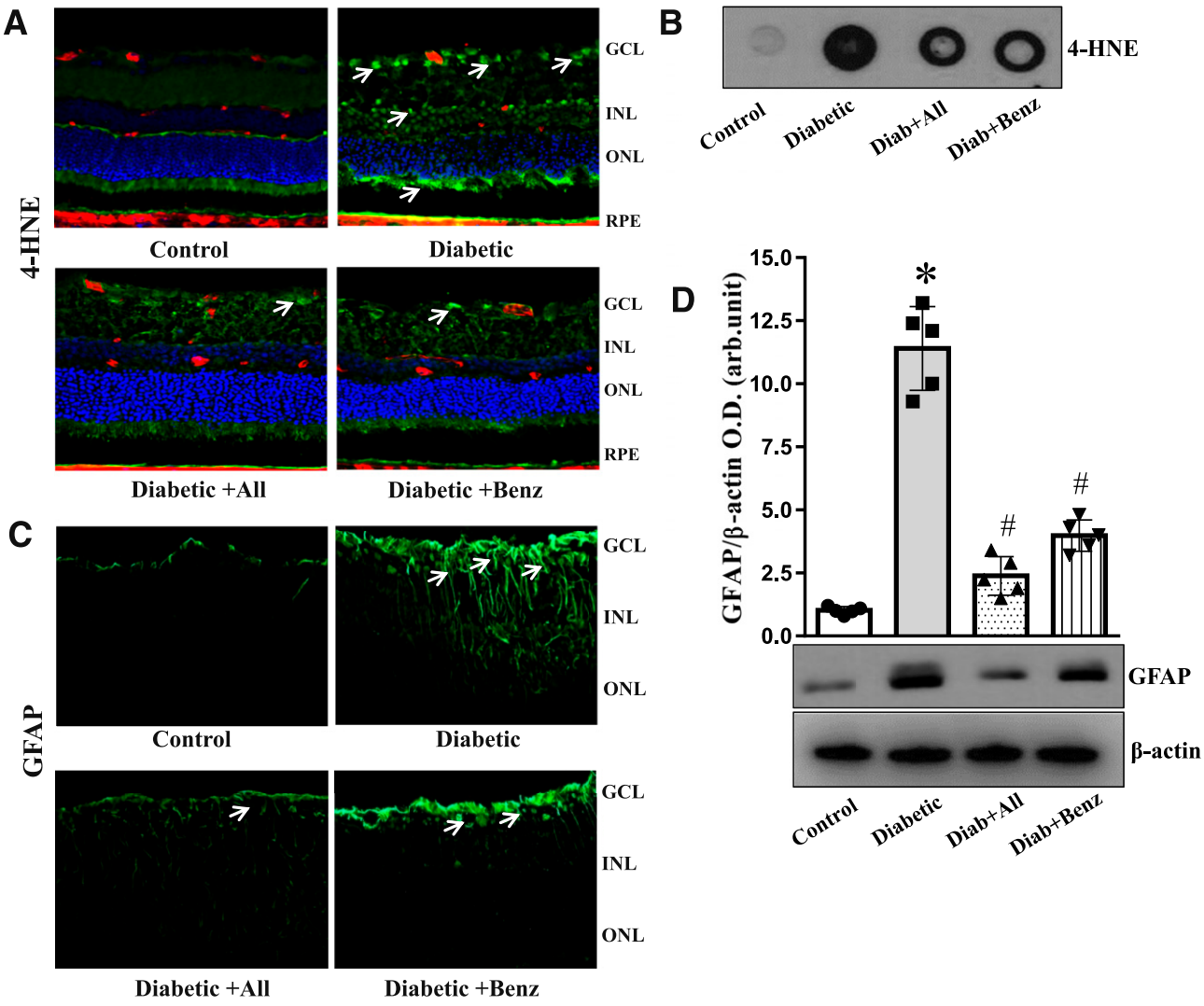

Figure 7—Effects of hypouricemic drugs on 4-HNE and GFAP expression. *A*: Immunohistochemical analysis of 4-HNE (green) in retinas of control rats (Control), STZ-rats (Diabetic), and STZ-rats treated with allopurinol (Diabetic+All) or benzbromarone (Diabetic+Benz). Sections were colabeled with isolectin B4 (red) for detection of vascular structures. Hoechst staining was used for nuclear counterstain (blue). White arrows indicate 4-HNE–positive cells. GCL, ganglion cell layer; INL, inner nuclear layer; ONL, outer nuclear layer. *B*: Dot blot analysis of 4-HNE in retinal tissue of control rats, STZ-rats, and STZ-rats treated with allopurinol (Diab+All) or benzbromarone (Diab+Benz). *C*: Representative images for GFAP immunoreactivity in control rats, STZ-rats, and STZ-rats treated with allopurinol and benzbromarone. White arrows indicate GFAP-positive cells. *D*: GFAP protein levels determined by Western blot analysis in retinal tissue in control rats, STZ-rats, and STZ-rats receiving allopurinol or benzbromarone. Bar histograms are representative of measurements of the optical density (O.D.) of GFAP-specific immunoreactivity normalized vs. β-actin. Data are mean ± SD; $n = 6$; *$P < 0.001$ vs. Control; #$P < 0.001$ vs. Diabetic.

examined the effects of diabetes and hypouricemic drugs on diabetes-induced activation of the NLRP3 inflammasome by assessing the expression levels of its constituents. As shown in Fig. 8, administration of allopurinol and benzbromarone effectively reduced hyperglycemia-induced expression of NLRP3 (Fig. 8*A*) and TLR4 (Fig. 8*B*) in rat retinas after 8 weeks of diabetes ($P < 0.01$; $n = 6$). In all experimental conditions, changes in TLR4 and NLRP3 retinal expression levels positively correlated with levels of IL-1β that we have measured in retinal extracts (Fig. 4), further confirming that specific relationship between UA levels and induction of sterile inflammation.

Furthermore, we analyzed the expression of NLRP3 inflammasome constituents in postmortem retinas of donors with and without diabetes. Immunoblotting analysis showed a significant upregulation in protein levels of NLRP3 ($P < 0.01$; $n = 8$) (Fig. 8*D*) and TLR4 ($P < 0.01$; $n = 8$) (Fig. 8*E*) in donors with DR compared with control donors without diabetes. In particular, ELISA assay measuring IL-1β in retinal lysates of donors with DR showed a 4.1-fold increase in levels of this cytokine ($P < 0.05$; $n = 8$) (Fig. 8*F*), and correlation analysis demonstrated a positive relationship of these values with UA vitreous levels ($R^2 = 0.75$, $P < 0.01$; $n = 8$) (Fig. 8*F*), thus confirming that

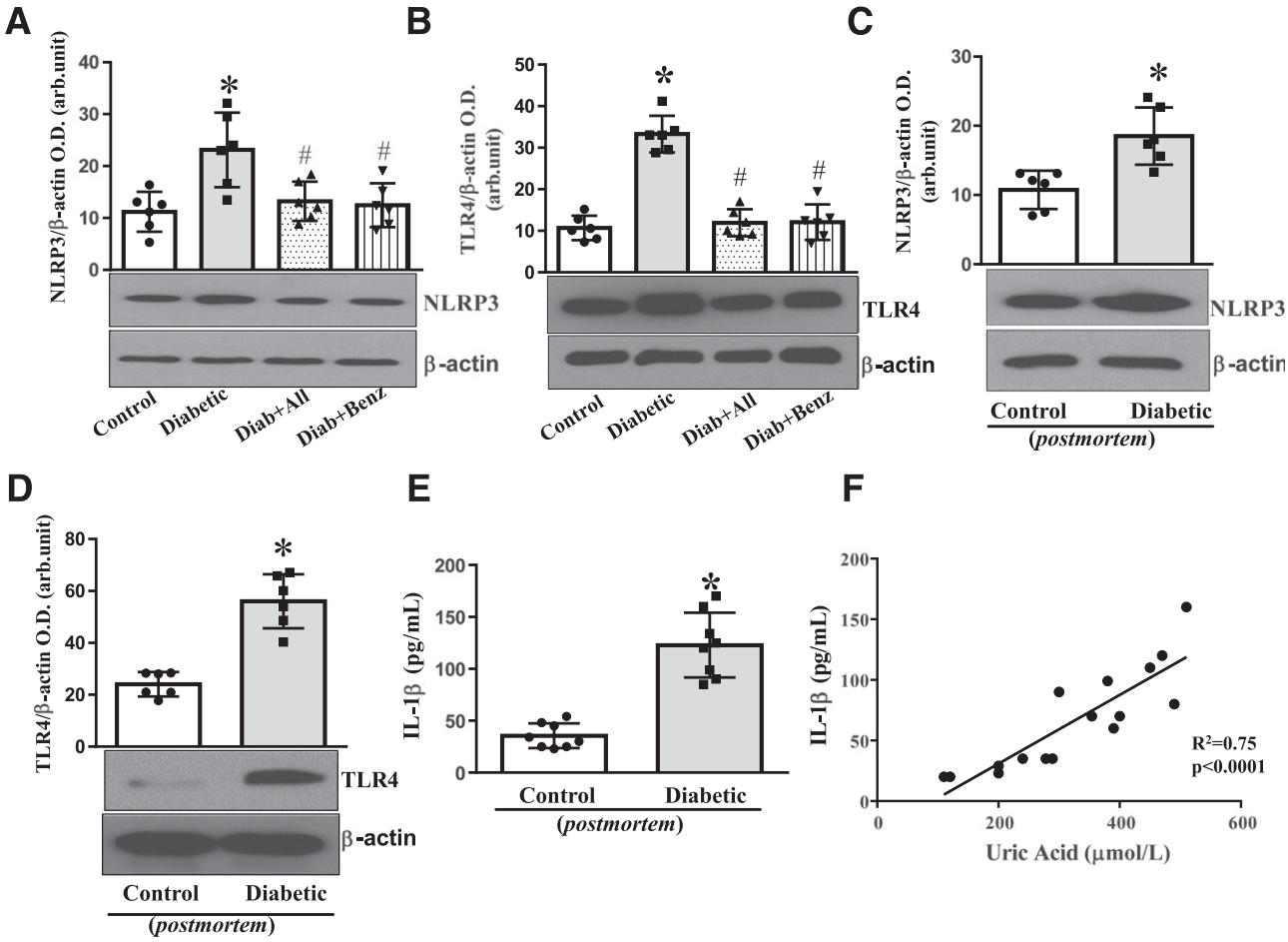

Figure 8—Effects of UA-lowering drugs on inflammasome activation. *A* and *B*: Western blot analysis showing NLRP3 (*A*) and TLR4 (*B*) specific immunoreactivity in retinal extracts of control rats (Control), STZ-rats (Diabetic), and STZ-rats receiving allopurinol (Diab+All) or benzbromarone (Diab+Benz). Optical density (O.D.) values of NLRP3 and TLR4 protein levels relative to β-actin are represented in bar histograms. Data are mean ± SD; $n = 6$. *$P < 0.01$ vs. Control; #$P < 0.05$ vs. Diabetic. *C* and *D*: Western blot analysis of NLRP3-specific (*C*) and TLR4-specific (*D*) immunoreactivity in retinas of postmortem normoglycemic donors (Control) and donors with DR (Diabetic). Bar histograms are representing measures of optical density normalized vs. β-actin. *$P < 0.01$ vs. Control. *E*: Quantification of IL-1β production in vitreous samples of control donors and donors with DR. Concentrations are represented as a bar histogram. Data are mean ± SD; $n = 8$. *$P < 0.001$ vs. Control. *F*: The correlation analysis between serum UA levels and IL-1β in postmortem samples of DR and control donors ($R^2 = 0.75$; $P < 0.001$; $n = 16$).

activation of autoinflammatory processes (sterile inflammation) in the retina of individuals with diabetes is directly associated with elevated vitreous levels of UA.

DISCUSSION

We investigated the contribution of MSU, the crystal form of UA, to retinal inflammation and progression to DR. To date, hyperglycemia, hypertension, and hyperlipidemia have been considered main risk factors for DR, and their clinical management represents a main therapeutic goal (44). New evidence, however, has suggested that monitoring inflammatory mediators in patients with diabetes may hold important adjunctive value as predictors of occurrence and progression of diabetic complications, including retinopathy (3,38).

UA is a by-product of purine oxidative catabolism by XOD (45). Excessive UA levels cause the human disease of gout, which is characterized by systemic inflammatory processes (18). Recent clinical studies have pointed out that a modest elevation in the "normal-high" range (6–8 mg/dL [357–476 μmol/L]) of UA blood levels is strongly associated with adverse cardiovascular outcomes, metabolic syndrome, diabetes, and progression of diabetic nephropathy (8,13,14,24–27). Despite few studies reporting enhanced UA levels in the vitreous of patients affected by diabetic macular edema (30,46), no further clinical investigation has been conducted to determine the potential contribution of UA to DR.

Here, we report that levels of UA were elevated in vitreous of postmortem human donors with DR and also in freshly isolated vitreous samples from patients with DR undergoing pars plana vitrectomy. Although preliminary, these results in human DR further confirm previous observations (30,47) and indicate the need for much

larger clinical studies. Furthermore, in an experimental model of type 1 diabetes, STZ-rats, we found that hyperglycemia promotes an elevation in serum and vitreous levels of UA compared with age-matched normoglycemic controls.

The presence of UA in the normal vitreous may exert beneficial effects through its antioxidant ability (48). However, in the diabetic condition, the UA concentration arises above the nucleation threshold value of 354 μmol/L (6 mg/dL), thus implying that most of the UA in these biological fluids exists in the form of MSU crystals (6). These are known irritants, which exert adverse biological activities by promoting pro-oxidative and proinflammatory effects (18,45).

Our data showed that allopurinol and benzbromarone both prevented retinal vascular permeability and leukostasis. These effects were associated with the ability of the hypouricemic drugs to reduce the expression of VEGF, ICAM-1, and other inflammatory cytokines and also with reduced oxidative/nitrative stress parameters.

The proinflammatory effects of MSU have been largely explained by its role as an alarmin (18) through activation of the NLRP3 inflammasome (17,19). Sterile inflammation underlies the development of cardiovascular disease (13) and of diabetic complications (26). Our data show that in STZ-rats, there was an upregulation of constituents of the NLRP3 inflammasome, including NLRP3, TLR4, and IL-1β, which was halted by UA-lowering drugs, thus establishing a cause-and-effect relationship between UA and sterile inflammation in the diabetic rat retina. Most importantly, our data analyzing human postmortem retinas further confirmed the involvement of sterile inflammation in UA/MSU proinflammatory activity by evidencing the upregulation of the NLRP3 inflammasome in postmortem donors with DR and demonstrating the existence of a positive correlation between IL-1β and UA vitreous levels in these samples.

Our studies further show that along with elevation of systemic UA/MSU levels, there is increased retinal production of this alarmin due to upregulation of XOD expression. In line with this evidence, allopurinol, which specifically blocks XOD (32), showed greater ability to prevent retinal inflammation than benzbromarone, which primarily exert systemic UA levels by increasing its urinary excretion (33). Additional effects of allopurinol may also involve decreased retinal oxidative stress due to XOD blockade (49).

In summary, our study suggests that monitoring of MSU levels may have important predictive and prognostic value for DR and warrant the realization of specific clinical studies to confirm uricemia as new risk factor for DR and validate the use of hypouricemic drugs as an adjunctive therapy for the treatment of this potentially blinding complication of diabetes.

Acknowledgments. The authors acknowledge the excellent technical assistance of Dr. Jianghe Yuan (Medical College of Georgia, Augusta University, Augusta, GA). The authors also thank Giovanni Parisi (IRCCS Fodazione G.B. Bietti, Rome, Italy) for his technical assistance for the human studies and the Facility for Complex Protein Mixture (CPM) (Istituto Superiore di Sanità, Rome, Italy).

Funding. This work received financial support from the International Retinal Research Foundation (to M.B.) and from the National Institutes of Health National Eye Institute (R01-EY-022416 and R01-EY-028714 to M.B.).

Duality of Interest. No potential conflicts of interest relevant to this article were reported.

Author Contributions. M.C.T. performed the experiments and developed the project. A.M. organized and performed the experiments with human samples. F.L.P. contributed to the in vivo experiments. P.M. participated in the in vitro and in vivo experiments. D.R.G. contributed to data analysis and manuscript preparation. A.B. analyzed human vitreous samples. G.R. provided the vitreous samples. A.R. provided the vitreous samples and clinical expertise for data analysis. A.T. performed and analyzed the FA data. P.M.M. contributed to data analysis and writing the manuscript. F.F. contributed to the realization of the human studies and data analysis. M.B. developed the idea, designed the studies described here, and provided financial support for their realization. M.B. is the guarantor of this work and, as such, had full access to all the data in the study and takes responsibility for the integrity of the data and the accuracy of the data analysis.

References

1. Antonetti DA, Klein R, Gardner TW. Diabetic retinopathy. N Engl J Med 2012; 366:1227–1239
2. Kiire CA, Porta M, Chong V. Medical management for the prevention and treatment of diabetic macular edema. Surv Ophthalmol 2013;58:459–465
3. Al-Shabrawey M, Rojas M, Sanders T, et al. Role of NADPH oxidase in retinal vascular inflammation. Invest Ophthalmol Vis Sci 2008;49:3239–3244
4. Roy MS, Janal MN, Crosby J, Donnelly R. Inflammatory biomarkers and progression of diabetic retinopathy in African Americans with type 1 diabetes. Invest Ophthalmol Vis Sci 2013;54:5471–5480
5. Sabán-Ruiz J, Alonso-Pacho A, Fabregate-Fuente M, de la Puerta González-Quevedo C. Xanthine oxidase inhibitor febuxostat as a novel agent postulated to act against vascular inflammation. Antiinflamm Antiallergy Agents Med Chem 2013; 12:94–99
6. Grassi D, Ferri L, Desideri G, et al. Chronic hyperuricemia, uric acid deposit and cardiovascular risk. Curr Pharm Des 2013;19:2432–2438
7. Meneshian A, Bulkley GB. The physiology of endothelial xanthine oxidase: from urate catabolism to reperfusion injury to inflammatory signal transduction. Microcirculation 2002;9:161–175
8. Dehghan A, van Hoek M, Sijbrands EJ, Hofman A, Witteman JC. High serum uric acid as a novel risk factor for type 2 diabetes. Diabetes Care 2008;31:361–362
9. Watanabe S, Kang DH, Feng L, et al. Uric acid, hominoid evolution, and the pathogenesis of salt-sensitivity. Hypertension 2002;40:355–360
10. Shi Y, Evans JE, Rock KL. Molecular identification of a danger signal that alerts the immune system to dying cells. Nature 2003;425:516–521
11. Punzi L, So A. Serum uric acid and gout: from the past to molecular biology. Curr Med Res Opin 2013;29(Suppl. 3):3–8
12. Goldfinger SE. Treatment of gout. N Engl J Med 1971;285:1303–1306
13. Chen CC, Hsu YJ, Lee TM. Impact of elevated uric acid on ventricular remodeling in infarcted rats with experimental hyperuricemia. Am J Physiol Heart Circ Physiol 2011;301:H1107–H1117
14. Heinig M, Johnson RJ. Role of uric acid in hypertension, renal disease, and metabolic syndrome. Cleve Clin J Med 2006;73:1059–1064
15. Maetzler W, Stapf AK, Schulte C, et al. Serum and cerebrospinal fluid uric acid levels in Lewy body disorders: associations with disease occurrence and amyloid-β pathway. J Alzheimers Dis 2011;27:119–126
16. Dunne A. Inflammasome activation: from inflammatory disease to infection. Biochem Soc Trans 2011;39:669–673
17. Kono H, Chen CJ, Ontiveros F, Rock KL. Uric acid promotes an acute inflammatory response to sterile cell death in mice. J Clin Invest 2010;120:1939–1949

18. Ghaemi-Oskouie F, Shi Y. The role of uric acid as an endogenous danger signal in immunity and inflammation. Curr Rheumatol Rep 2011;13:160–166
19. Hornung V, Bauernfeind F, Halle A, et al. Silica crystals and aluminum salts activate the NALP3 inflammasome through phagosomal destabilization. Nat Immunol 2008;9:847–856
20. Martinon F, Pétrilli V, Mayor A, Tardivel A, Tschopp J. Gout-associated uric acid crystals activate the NALP3 inflammasome. Nature 2006;440:237–241
21. Franchi L, Warner N, Viani K, Nuñez G. Function of Nod-like receptors in microbial recognition and host defense. Immunol Rev 2009;227:106–128
22. Reynolds CM, McGillicuddy FC, Harford KA, Finucane OM, Mills KH, Roche HM. Dietary saturated fatty acids prime the NLRP3 inflammasome via TLR4 in dendritic cells-implications for diet-induced insulin resistance. Mol Nutr Food Res 2012;56:1212–1222
23. Gurung P, Malireddi RK, Anand PK, et al. Toll or interleukin-1 receptor (TIR) domain-containing adaptor inducing interferon-β (TRIF)-mediated caspase-11 protease production integrates Toll-like receptor 4 (TLR4) protein- and Nlrp3 inflammasome-mediated host defense against enteropathogens. J Biol Chem 2012;287:34474–34483
24. Rodrigues TC, Maahs DM, Johnson RJ, et al. Serum uric acid predicts progression of subclinical coronary atherosclerosis in individuals without renal disease. Diabetes Care 2010;33:2471–2473
25. Magri CJ, Calleja N, Buhagiar G, Fava S, Vassallo J. Factors associated with diabetic nephropathy in subjects with proliferative retinopathy. Int Urol Nephrol 2012;44:197–206
26. Bhole V, Choi JW, Kim SW, de Vera M, Choi H. Serum uric acid levels and the risk of type 2 diabetes: a prospective study. Am J Med 2010;123:957–961
27. Jalal DI, Rivard CJ, Johnson RJ, et al. Serum uric acid levels predict the development of albuminuria over 6 years in patients with type 1 diabetes: findings from the Coronary Artery Calcification in Type 1 Diabetes study. Nephrol Dial Transplant 2010;25:1865–1869
28. Abraham A, Breiner A, Barnett C, et al. Uric acid levels correlate with the severity of diabetic sensorimotor polyneuropathy. J Neurol Sci 2017;379: 94–98
29. Lin X, Xu L, Zhao D, Luo Z, Pan S. Correlation between serum uric acid and diabetic peripheral neuropathy in T2DM patients. J Neurol Sci 2018;385: 78–82
30. Krizova L, Kalousova M, Kubena A, et al. Increased uric acid and glucose concentrations in vitreous and serum of patients with diabetic macular oedema. Ophthalmic Res 2011;46:73–79
31. Devi TS, Lee I, Hüttemann M, Kumar A, Nantwi KD, Singh LP. TXNIP links innate host defense mechanisms to oxidative stress and inflammation in retinal Muller glia under chronic hyperglycemia: implications for diabetic retinopathy. Exp Diabetes Res 2012;2012:438238
32. Szasz T, Linder AE, Davis RP, Burnett R, Fink GD, Watts SW. Allopurinol does not decrease blood pressure or prevent the development of hypertension in the deoxycorticosterone acetate-salt rat model. J Cardiovasc Pharmacol 2010;56: 627–634
33. Schwartz IF, Grupper A, Chernichovski T, et al. Hyperuricemia attenuates aortic nitric oxide generation, through inhibition of arginine transport, in rats. J Vasc Res 2011;48:252–260
34. Thounaojam MC, Powell FL, Patel S, et al. Protective effects of agonists of growth hormone-releasing hormone (GHRH) in early experimental diabetic retinopathy. Proc Natl Acad Sci U S A 2017;114:13248–13253
35. Liu Q, Li J, Cheng R, et al. Nitrosative stress plays an important role in Wnt pathway activation in diabetic retinopathy. Antioxid Redox Signal 2013;18:1141–1153
36. Moriwaki Y, Yamamoto T, Higashino K. Enzymes involved in purine metabolism–a review of histochemical localization and functional implications. Histol Histopathol 1999;14:1321–1340
37. McLeod DS, Lefer DJ, Merges C, Lutty GA. Enhanced expression of intracellular adhesion molecule-1 and P-selectin in the diabetic human retina and choroid. Am J Pathol 1995;147:642–653
38. Kern TS. Contributions of inflammatory processes to the development of the early stages of diabetic retinopathy. Exp Diabetes Res 2007;2007:95103
39. Joussen AM, Poulaki V, Mitsiades N, et al. Nonsteroidal anti-inflammatory drugs prevent early diabetic retinopathy via TNF-alpha suppression. FASEB J 2002;16:438–440
40. Joussen AM, Poulaki V, Le ML, et al. A central role for inflammation in the pathogenesis of diabetic retinopathy. FASEB J 2004;18:1450–1452
41. Giacco F, Brownlee M. Oxidative stress and diabetic complications. Circ Res 2010;107:1058–1070
42. Yun MR, Park HM, Seo KW, Lee SJ, Im DS, Kim CD. 5-Lipoxygenase plays an essential role in 4-HNE-enhanced ROS production in murine macrophages via activation of NADPH oxidase. Free Radic Res 2010;44:742–750
43. Uchida K. 4-Hydroxy-2-nonenal: a product and mediator of oxidative stress. Prog Lipid Res 2003;42:318–343
44. Harris Nwanyanwu K, Talwar N, Gardner TW, Wrobel JS, Herman WH, Stein JD. Predicting development of proliferative diabetic retinopathy. Diabetes Care 2013;36:1562–1568
45. Ardan T, Kovaceva J, Cejková J. Comparative histochemical and immunohistochemical study on xanthine oxidoreductase/xanthine oxidase in mammalian corneal epithelium. Acta Histochem 2004;106:69–75
46. Mohora M, Vîrgolici B, Coman A, et al. Diabetic foot patients with and without retinopathy and plasma oxidative stress. Rom J Intern Med 2007;45:51–57
47. Krizova L, Kalousova M, Kubena AA, et al. Correlation of vitreous vascular endothelial growth factor and uric acid concentration using optical coherence tomography in diabetic macular edema. J Ophthalmol 2015;2015:478509
48. Ames BN, Cathcart R, Schwiers E, Hochstein P. Uric acid provides an antioxidant defense in humans against oxidant- and radical-caused aging and cancer: a hypothesis. Proc Natl Acad Sci U S A 1981;78:6858–6862
49. Goharinia M, Zareei A, Rahimi M, Mirkhani H. Can allopurinol improve retinopathy in diabetic rats? Oxidative stress or uric acid; which one is the culprit? Res Pharm Sci 2017;12:401–408